Petroleum Science 20 (2023) 474–481

Contents lists available at ScienceDirect

Petroleum Science

journal homepage: www.keaipublishing.com/en/journals/petroleum-science

Original Paper

Experimental research on the contact force of the bi-directional pig in oil and gas pipeline

Xiao-Xiao Zhu*, Chun-Ming Fu, Yu-Tao Wang, Shi-Ming Zhang

College of Mechanical and Transportation Engineering, China University of Petroleum-Beijing, Changping, Beijing, 102249, China

ARTICLE INFO

Article history:
Received 14 February 2022
Received in revised form
16 August 2022
Accepted 17 August 2022
Available online 27 August 2022

Edited by Xiu-Qiu Peng

Keywords:
Pipeline pig
Sealing disc
Contact force
Friction coefficient
Experimental rig

ABSTRACT

The migration process of the pig in oil and gas pipeline is a complex dynamic problem. During the pigging operation, the variation of friction force caused by the nonlinear contact between the sealing disc and the pipe wall is the key factor affecting the dynamic characteristics of the pig motion. At present, the existed pigging models for predicting pigging behavior regard friction as an invariant constant. Experimental research indicates that the friction force of the pig varies with the contact force and the lubrication conditions. Therefore, the assumption that the friction force is constant cannot reflect the friction dynamic characteristics of the pig during pigging, and will also affect the accuracy of the pigging model. Exploring the variation of friction force of pig under different conditions is the basis of establishing the transient dynamic model of a pig. As a result, in this paper, a method of direct measurement of contact force between the pig and the pipeline is presented, the contact force, the friction force, as well as the friction coefficient of the pig are obtained from the experiment. Research results in this paper can help to establish a more accurate dynamic model of pig.

1. Introduction

The rapid growth of oil and gas demand has promoted the development of pipeline transportation industry. Along with the increase of the pipeline service life, problems such as wax deposition, pipeline corrosion and deformation often occur. It is necessary to clean and inspect the pipeline regularly to ensure the safe and efficient operation of the pipeline Tiratsoo (1992); Tiratsoo (2013); (Azevedo et al., 1996; Azevedo et al., 1996; Niechele et al., 2000).

Pipeline inspection gauge(pig) is the general term for pipeline pigging and testing (Quarini and Shire, 2007; Saeidbakhsh et al., 2009). There are different types of pigs, and can be classified by their maintenance aim: routine pigging for keeping a pipeline free of sediments and/or moisture; geometry inspections to ensure that a pipeline is free from major physical damages; intelligent pigging, for delivering detailed information about a pipeline (Sadovnychiy and Lopez, 2005; Rahe, 2006). Sealing discs are important component and commonly used on pig due to the high-efficient sealing and excellent pigging ability. These sealing discs with outer diameter slightly larger than the pipeline inner diameter contact the inner wall of the pipeline and seal the pipeline, so as to form the pressure difference before and after the pig and push it forward (Botros and Golshan, 2009; Esmaeilzadeh et al., 2009). Due to the elasticity of the sealing discs, the interaction between the sealing discs and the pipeline will directly affect the friction force between sealing disc and pipeline (Zhu et al., 2015; Zhang et al., 2015; Zhang et al., 2022).

The friction force between sealing disc and pipeline is one of the key factors in determining the characteristics of a pig motion (Zhang et al., 2020). As a result, it is important to understand the friction force between rubber and pipe wall for studying and understanding pigging movement (Liu et al., 2021; Tan et al., 2014). However, the hyperelastic, time-and temperature-dependent material behaviour of rubber, the sliding velocity and the presence of lubricants make the tribology of pig a challenging research area (Zhu et al., 2017; Liu et al., 2020). So far, few models can be used to estimate the transient friction force during pipeline pigging. Prediction usually depends on experimental results and field experience, which with highly uncertainty (Lesani et al., 2012; Bódai and Goda, 2014; Patricio et al., 2020). The current pigging model often fails to simulate the locally occurring speed excursion in detail due to the difficulty of predicting the variations in friction force between the pig and pipe wall (Kim et al., 2022). Variation of contact

* Corresponding author.
E-mail address: x.zhu@cup.edu.cn (X.-X. Zhu).

https://doi.org/10.1016/j.petsci.2022.08.021

force between the pig and the pipeline wall during pigging is an important factor for the transient change of the frictional force and clearly understand the contact force will be essential for building an accurate friction model (Van Spronsen et al., 2013; de Souza et al., 2013).

A mathematical model for evaluating the contact force of a bidirectional pig was proposed (O'Donoghue, 1996). Due to assumption that the deformed sealing disc was an ideal arc, the equations proposed for estimating the geometrical deformation of the sealing discs were simplified and the friction force was underpredicted. In order to improve the accuracy of the contact force predicting result, nonlinear finite element model (FEM) was proposed to estimate the contact force of a bidirectional pig (Zhu et al., 2015). A pull test in which a sealing disc pig is pulled through a pipe while monitoring the pulling force was conducted for measuring the friction force. The contact force was evaluated and verified according to the Coulomb's law of friction with the assumption that the friction coefficient is a constant value. However, friction coefficient is not a constant value, and it varies with the variation of contact force, pipe wall roughness, lubrication and so on (Persson, 2001; Zhu et al., 2017). If the contact force can be experimental obtained, the friction coefficient can be experimental investigated as well. As a result, how to measure the contact force with high accuracy becomes an interesting topic, and arose more attention.

An experimental facility to measure the wall force was proposed (Hendrix et al., 2016; Den Heijer, 2016). A steel hull was wrapped around the sealing disk, different oversize can be modeled by reducing the diameter of the steel plate, and the force for reducing the diameter was measured by a load cell, which can be finally transferred to contact force. In order to prevent the disc slides in the axial direction, a 2 mm steel ring has been welded onto the wrapped hull. Also, the deformation of the sealing disc is measured by using a profile comb mounting on the spacer disc (Hendrix et al., 2018). However, this is still not an ideal method since the contact force was transferred from the force for reducing the diameter of hull, which can also bring error. In order to experimental investigate the contact force with higher accuracy, a more convenient and intuitive method is proposed to directly measure the contact force by extending the sensor probe into the pipe wall, and the overall contact force of the sealing disc can be obtained after calculation. Since the contact force and the friction force can all obtained according to the rig, the friction coefficient can finally be in situ measured. Research in this paper can help to have a better understanding of the contact force and the friction force of a pig.

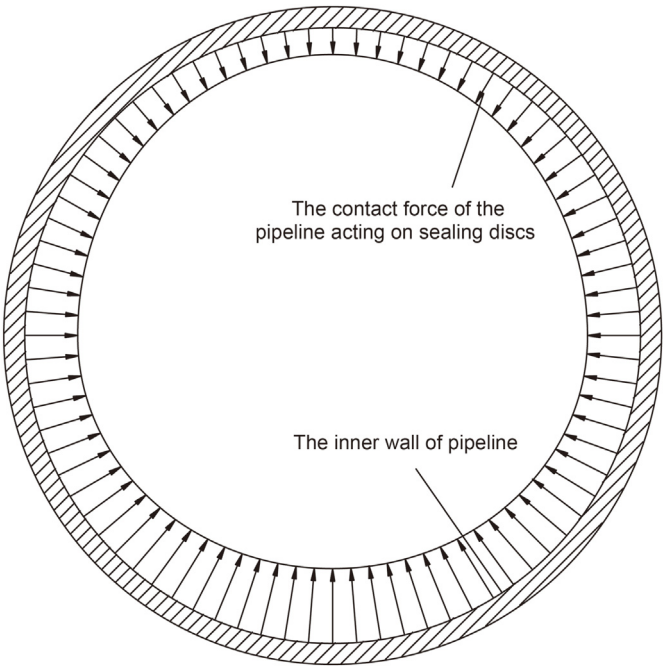

Fig. 1. Gravity induced contact force distribution profile (Zhu et al., 2015).

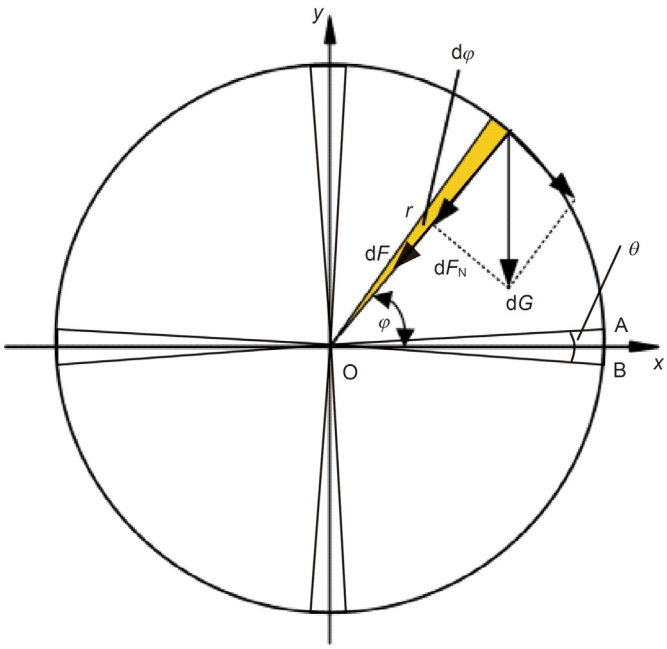

Fig. 2. Force analysis on the effect of the pig's gravity on the deformed sealing disc.

2. Mathematical model

As shown in Fig. 1 The diameter of the sealing disc is slightly larger than the pipeline inner diameter, which is interference fit with the pipe wall. Due to the pig's gravity, contact force between the sealing disc and the pipe wall is non-uniform distributed. The upper half of the sealing disc undergoes a larger deformation than the lower half. Therefore, the contact force at the top is smaller than that at the bottom.

As shown in Fig. 2, the sealing disc is divided into infinite equal parts in the circumferential direction, and the contact force from each part can be expressed in Eq. (1)

$$dF = \frac{F}{2\pi}d\varphi + \frac{G}{2\pi}\sin\varphi d\varphi \tag{1}$$

where F is the overall contact force, dF is the contact force of the selected infinitesimal part, G is the gravity of the pig, φ is the angle between the selected infinitesimal part and the horizontal line, the

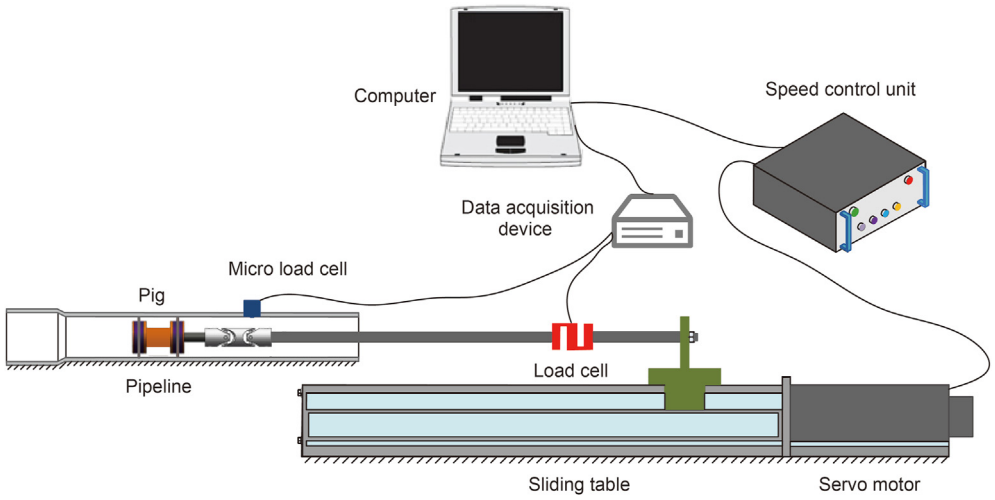

Fig. 3. Schematic diagram of contact force and friction force test device.

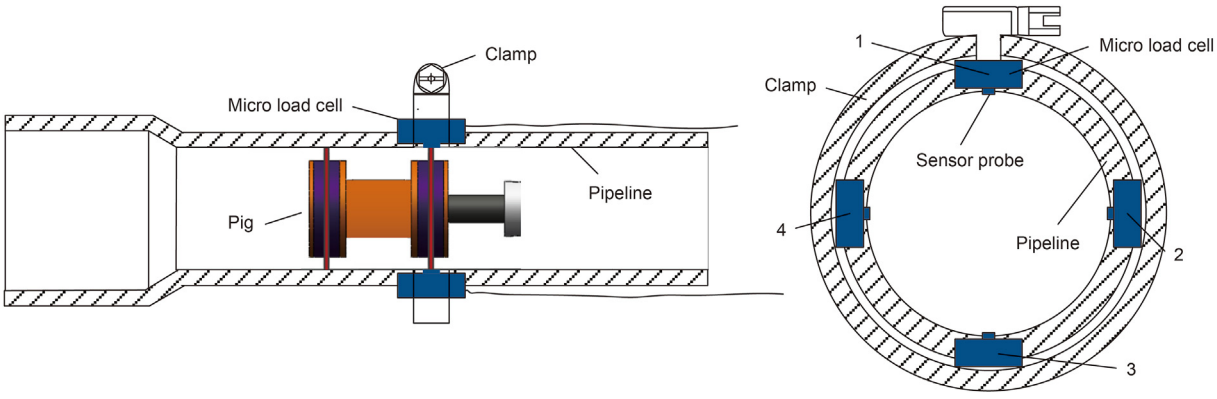

Fig. 4. Layout of the micro load cell sensors for measuring the contact force.

$d\varphi$ is the central angle of the selected infinitesimal part.

The sensor probes were arranged to place on 3, 6, 9, 12 o'clock position of the pipe (see in Fig. 4), and the diameter of the probe is 3 mm, which means the contact length of AB in Fig. 2 is 3 mm. θ is the angle between the positive x-axis direction and OA ($\angle AOX = \theta$, and $\angle AOB = 2\theta$). Then, the contact forces directly detected at the four points are supposed to be obtained according to Eq. (2):

$$F_3 = \int_{-\theta}^{\theta} dF = \int_{-\theta}^{\theta} \frac{F}{2\pi} d\varphi - \frac{G}{2\pi} \sin\varphi d\varphi$$

$$F_6 = \int_{-\theta+\frac{3\pi}{2}}^{\theta+\frac{3\pi}{2}} dF = \int_{-\theta+\frac{3\pi}{2}}^{\theta+\frac{3\pi}{2}} \frac{F}{2\pi} d\varphi + \frac{G}{2\pi} \sin\varphi d\varphi = \int_{-\theta}^{\theta} \frac{F}{2\pi} d\varphi + \frac{G}{2\pi} \sin\varphi d\varphi$$

$$F_9 = \int_{-\theta+\pi}^{\theta+\pi} dF = \int_{-\theta}^{\theta} \frac{F}{2\pi} d\varphi - \frac{G}{2\pi} \sin\varphi d\varphi$$

$$F_{12} = \int_{-\theta+\frac{\pi}{2}}^{\theta+\frac{\pi}{2}} dF = \int_{-\theta+\frac{\pi}{2}}^{\theta+\frac{\pi}{2}} \frac{F}{2\pi} d\varphi - \frac{G}{2\pi} \sin\varphi d\varphi = \int_{-\theta}^{\theta} \frac{F}{2\pi} d\varphi - \frac{G}{2\pi} \sin\varphi d\varphi \quad (2)$$

where F_3, F_6, F_9, F_{12} are the detected forces at 3, 6, 9, 12 o'clock position of the pipe, θ is the half-angle radian value of the measurement point, and its magnitude can be obtained from Eq. (3):

$$\theta = \frac{1}{2} \arcsin \frac{AB}{r} \quad (3)$$

where r is the radius of the sealing disc.

From Eqs. (2) and (3), it can be found that the contact force can be obtained once any one of these four measuring points are detected, and the total contact force can be expressed in Eq. (4):

$$F = \frac{2\pi F_3}{2\theta} = \frac{2\pi F_6}{2\theta} - \frac{G}{\theta}\cos\theta = \frac{2\pi F_9}{2\theta} = \frac{2\pi F_{12}}{2\theta} + \frac{G}{\theta}\cos\theta \quad (4)$$

3. Experimental setup

An experimental rig is set up for directly measuring the contact force, as well as the friction force. The experimental platform is composed of motor, slide table, horizontal test pipe, micro load cell sensor, speed controller and data acquisition unit, as shown in Fig. 3. The slide table is built on the precision roller screw and can be driven uniformly under the motor. The drag force measured by the sensor directly connected to the pigging device is equal to the frictional force of the pig.

Schematic diagram of contact force test device is detailed shown

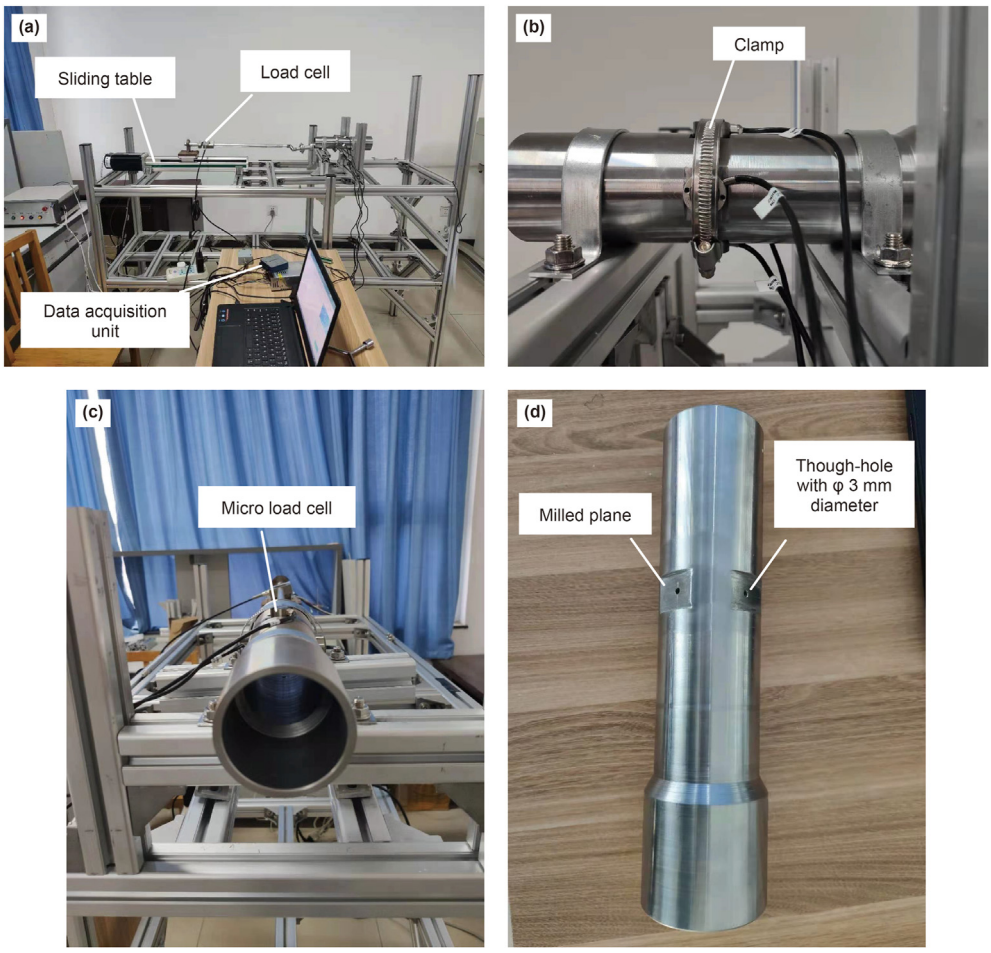

Fig. 5. Prototype of the experimental rig.

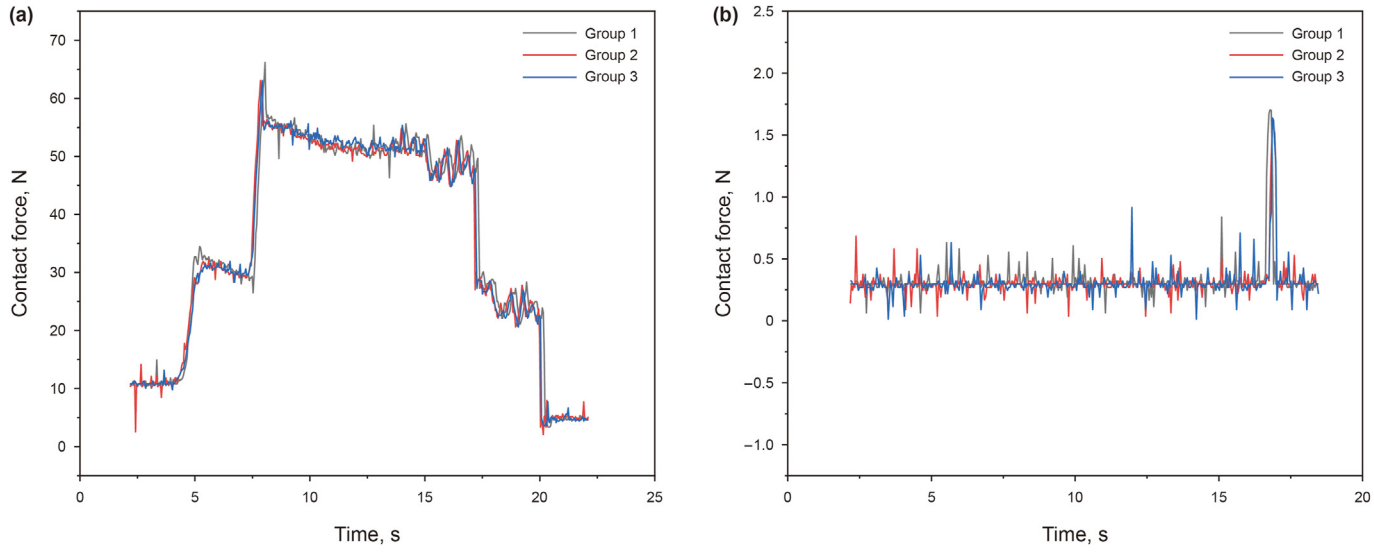

Fig. 6. Repeatability verification of the experimental results.

Table 1
Sealing discs' sizes used in the experiment and simulation.

Parameter	Outer diameter of the sealing discs (*Ds*)	Thickness of the sealing discs (*t*)	Outer diameter of separating discs (*dp*)
Value range (mm)	51–57	1–5	35–45
Inner diameter of the pipeline (*d*, mm)	50		
Interference (δ)[a]	2%–14%		
Thickness per pipeline inner diameter (ξ)[b]		2–10%	
Clamping rate (ζ)[c]			70%–90%

[a] Interference $\delta = (Ds - d)*100/d$, where *Ds* is the outer diameter of the sealing disc, *d* is the inner diameter of the pipeline.
[b] Thickness per pipeline inner diameter $\xi = t*100/d$, where *t* is the thickness of the sealing disc.
[c] Clamping rate $\zeta = dp*100/d$, where *dp* is the outer diameter of the clamping plate.

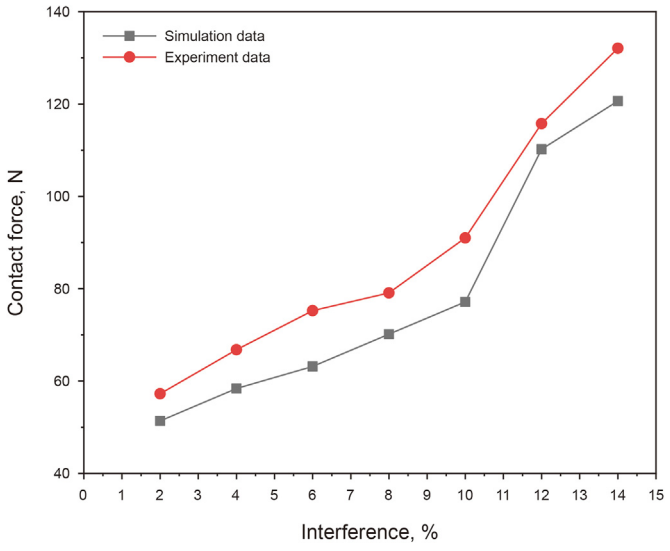

Fig. 7. Variation of contact force of the sealing disc with different interferences.

in Fig. 4. The pipe used in the experiment are customized steel pipe, the inner diameter of the pipe is 50 mm, and the pipe wall thickness is 5 mm. Four planes are milled at 3, 6, 9, 12 o 'clock position of the pipe for installing the micro load cell sensor (Fig. 5d), and the sizes of the planes are 20.5 mm × 20.5 mm. A though-hole with φ3 mm diameter is drilled at the center of each milled plane for the insertion of the sensor probe. After installation, the tip of the sensor probe is almost on the same surface with the inner wall of the pipe (0.05–0.10 mm out from the hole for detection). These four sensors are fixed with clamp, as shown in Fig. 4, and the photos of the experiment are shown in Fig. 5.

In the experiment, when the pig is dragging in the pipe, the deformed sealing disc can pass the detection point, the contact force resulted from the interference deformation of the sealing disc will directly act on the sensor probe. The data acquisition device connected to the sensor will monitor and collect the experimental data in real time. The measurement results deduced from the results of four sensors will be averaged to obtain an accurate contact force. The repeatability of the experimental data was investigated and verified. Three group of experiments were carried out under the same conditions, and it indicates that the reproducibility of the experimental results can be guaranteed, as shown in Fig. 6.

4. Comparison of the experimental and simulation results

Nonlinear simulation has been conducted before to investigate the contact force (Zhu et al., 2015). Since the contact force can be directly obtained here, in this section, the experimental results are compared with the simulation results to further verify the accuracy of the model built by finite elemental method. The variable parameters used in this experiment are the diameter of the sealing disc, the thickness of the sealing disc and the outer diameter of the clamping disc, as shown in Table 1.

4.1. Contact force of the sealing disc with different interferences

Comparison of the contact force between the experimental results and the simulation results are shown in Fig. 7. As the contact force of the pig is perpendicular to the pipe wall, it is found that with the increase of interference, the contact force of the pig increases linearly with the interference. When the interference of the sealing disc increases from 2% to 14%, the contact force increases from 51.38 N to 120.67 N in simulation, and from 57.26 N to 132.12 N in experiment. Compared with the experimental results, 16.1% maximum relative error of simulation results can be found at 6% interference and minimum relative error of 4.8% found at 12% interference. Considering the probe is 0.05 mm–0.10 mm out from the pipe inner wall, the experimental results should be a little smaller than in Fig. 7 and the relative error between the experimental results and the simulation results can be smaller as well.

4.2. Contact force of the sealing disc with different clamping rates

Contact force of the sealing disc with different clamping rates is shown in Fig. 8. With the increase of clamping rate, the bending deformation of the sealing disc becomes difficult, thus affecting the value of contact force. An exponential relationship between the contact force and the clamping rate can be found. The sealing disc becomes difficult to deform at larger clamping rate. When the clamping rate increases from 70% to 90%, the contact force increases from 48.89 N to 220.34 N in simulation, increases by 350.73%. However, from the experimental aspect, the contact force increases by 227.87%, from 62.44 N to 204.72 N. The maximum relative error is 21.71% at 70% clamping rate and the minimum relative error is 2.18% at 86% clamping rate. Compared with the results of interference, it is obvious that the clamping rate has a greater influence on the contact force than the interference.

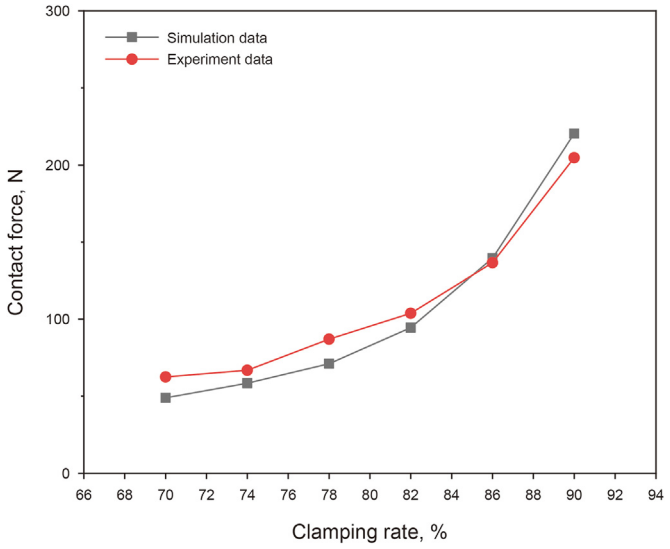

Fig. 8. Variation of contact force of the sealing disc with different clamping rates.

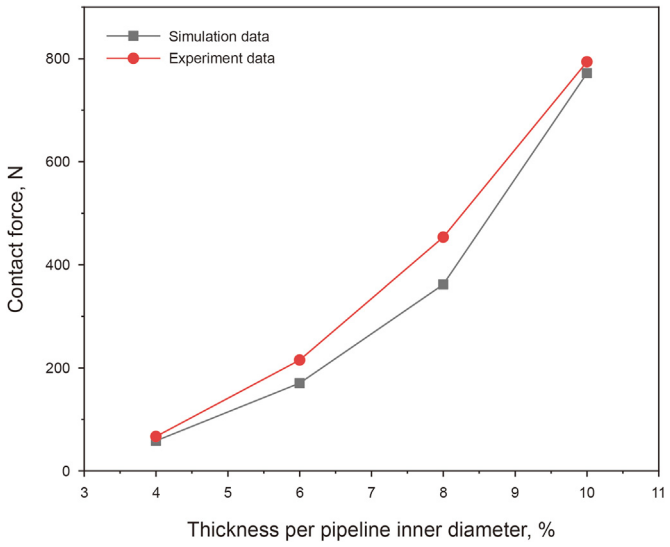

Fig. 9. Variation of contact force of the sealing disc with different thickness per pipeline inner diameters.

4.3. Contact force of the sealing disc with different thicknesses

A comparative analysis of the simulated contact force and the experimental contact force of the sealing disc with different thickness per pipeline inner diameters is shown in Fig. 9. The contact force of the pig increases with the increase of the thickness per pipeline inner diameter. When the thickness per pipeline inner diameter of the sealing disc increases from 4% to 10%, the contact force increases from 58.38 N to 771.79 N in simulation, contact force increased by 1221.99%. However, the contact force increased from 66.81 N to 794.00 N in experiment, contact force increased by 1088.46%. Compared with the experimental results, maximum relative error of 20.84% can be found at 6% thickness per pipeline inner diameter and minimum relative error of 2.80% found at 10% thickness per pipeline inner diameter in the simulation. It is obvious that the thickness per pipeline inner diameter has a far greater influence on the contact force than the interference and the clamping rate.

4.4. Friction coefficient

Since the contact force and the friction force can be detected by the experiment, the friction coefficient can be finally calculated. In the experiment, the running speed of the pig is 1000 mm/min and the inner wall of the pipe is completely dry. The inner surface roughness (Ra) of the pipeline was detected before the experiment and the roughness Ra is within 0.5–0.7 μm.

The variation trends of the friction coefficient of the pig with different interferences, clamping rates and thickness per pipeline inner diameters are shown in Fig. 10. The friction coefficient between the sealing disc and the pipe wall is within the range of 0.3–0.5. It can be found that the size of the sealing disc almost has no effect on the friction coefficient. The fluctuation of the friction coefficient can be neglected when the sealing disc has different interferences, clamping rates and thickness per pipeline inner diameters. As a result, it can be confirmed that the friction coefficient is mainly determined by the lubricant condition (velocity can also be classified into lubricant condition since the large velocity can change the temperature of the lubricant condition).

In simulation without considering the lubrication (Dry condition), the friction coefficient can be defined and input. However, the contact force resulted from the simulation almost has nothing to do with the friction coefficient, and the friction coefficient can only change the simulated friction force. Till now, FEM model for predicting the contact force of a bidirectional pig has been verified and proved to be effective. As long as the characteristics of the friction coefficient can be revealed in future, the friction force of the pig can be expressed clearly, as well as the dynamic pig motion. As a result, a further investigation on the friction coefficient is urgently needed.

5. Conclusions

This paper presents a method for directly measuring the contact force between the sealing disc and the pipe wall. The contact force of sealing disc is studied when the interference is within 2%–14%, the clamping rate is within 70%–90%, and the thickness per pipeline inner diameter is within 4%–10%. Because friction force can also be detected in this experimental rig, the friction coefficient between the sealing disc and the pipe wall of the pig is calculated and analyzed.

(1) The simulation model proposed for predicting the contact force and friction force is verified again according to the comparison of the experimental results. The comparison indicates that the maximum relative of 21.7% the simulation model can be found at 70% clamping rate.
(2) A parameter sensitivity of the sealing disc on the contact force has been investigated. Among the sizes of the sealing disc determining the contact force, the most influential parameter for contact force is the thickness per pipeline inner diameter, then the clamping rate. The influence of interference on contact force is far less than the other two parameters.
(3) The effects of the sealing disc's interference, the thickness per pipeline inner diameter, and the clamping rate on the friction coefficient are studied. The friction coefficient is

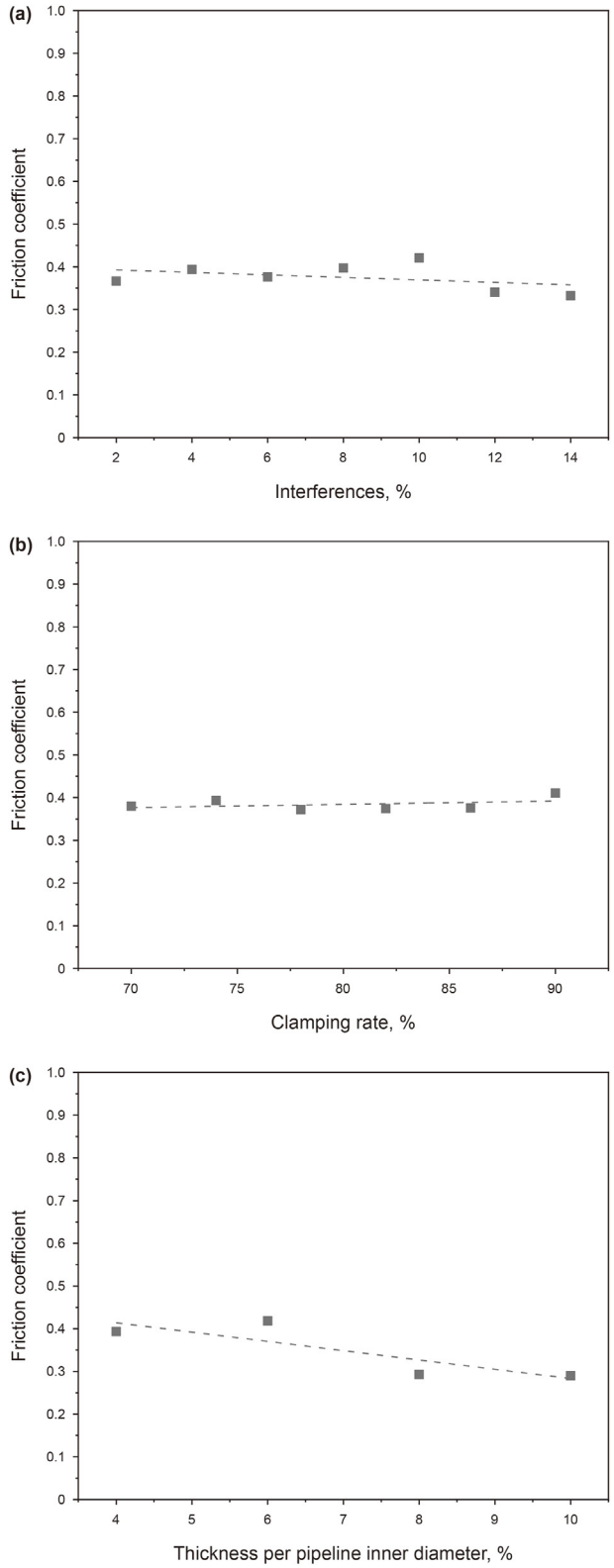

Fig. 10. Variation of friction coefficient of sealing disc with (**a**) different interferences, (**b**) clamping rates, (**c**) thickness per pipeline inner diameters.

mainly determined by the lubricant condition, and almost has nothing to do with the size of the sealing disc.

Acknowledgements

This work was supported by Science Foundation of China University of Petroleum, Beijing (No. 2462020YXZZ046, No. 2462020XKJS01), and the National Natural Science Foundation of China (No. 51509259).

References

Azevedo, L.F.A., Bracm, A.M.B., Nieckele, A.O., Naccxhe, M.F., Gomes, M.G., 1996. Simple hydrodynamic models for the prediction of pig motions in pipelines. In: Offshore Technology Conference. https://doi.org/10.4043/8232-MS, 6–9 May, Houston, Texas.

Bódai, G., Goda, T.J., 2014. Sliding friction of wiper blade: measurement, FE modeling and mixed friction simulation. Tribol. Int. 70, 63–74. https://doi.org/10.1016/j.triboint.2013.07.013.

Botros, K.K., Golshan, H., 2009. Dynamics of pig motion in gas pipelines. In: AGA-operations Conference and Biennial Exhibition. David L. Lawrence Convention, Pittsburgh, Pennsylvania. May.

de Souza, L.H.I., Silva, B.F., de Andrade, B.L.B., 2013. Analysis of contact forces acting upon pipelines pigs. In: COBEM 2013: 22nd International Congress of Mechanical Engineering, 3–7 November, Ribeirão Preto, SP, Brazil.

Den Heijer, A., 2016. Frictional Behaviour of Pigs in Motion. Delft University of Technology, Master Thesis.

Esmaeilzadeh, F., Mowla, D., Asemani, M., 2009. Mathematical modeling and simulation of pigging operation in gas and liquid pipelines. J. Petrol. Sci. Eng. 69 (1–2), 100–106. https://doi.org/10.1016/j.petrol.2009.08.006.

Hendrix, M.H.W., Den Heijer, A., Breugem, W.P., Henkes, R.A.W.M., 2016. Frictional forces during pigging of multiphase pipelines. In: 10th North American Conference on Multiphase Technology, 8–10 June, Banff, Canada.

Hendrix, M.H.W., Graafland, C.M., van Ostayen, R.A.J., 2018. Frictional forces for disc-type pigging of pipelines. J. Petrol. Sci. Eng. 171, 905–918. https://doi.org/10.1016/j.petrol.2018.07.076.

Kim, S., Yoo, K., Koo, B., Kim, D., Yoo, H., Seo, Y., 2022. Speed excursion simulation of PIG using improved friction models. J. Nat. Gas Sci. Eng. 97, 104371. https://doi.org/10.1016/j.jngse.2021.104371.

Lesani, M., Rafeeyan, M., Sohankar, A., 2012. Dynamic analysis of small pig through two and three-dimensional liquid pipeline. J. Appl. Fluid Mech. 5 (2), 75–83. https://doi.org/10.36884/jafm.5.02.12170.

Liu, C., Wei, Y., Cao, Y., Zhang, S., Sun, Y., 2020. Traveling ability of pipeline inspection gauge (PIG) in elbow under different friction coefficients by 3D FEM. J. Nat. Gas Sci. Eng. 75, 103134. https://doi.org/10.1016/j.jngse.2019.103134.

Liu, C., Cao, Y., Tian, H., Ma, S., 2021. A novel method for analyzing the driving force of the bi-directional pig based on the four-element model. Int. J. Pres. Ves. Pip. 190, 104314. https://doi.org/10.1016/j.ijpvp.2021.104314.

Niechele, A.O., Braga, A.M.B., Azevedo, L.F.A., 2000. Transient pig motion through non-isothermal gas and liquid pipelines. In: International Pipeline Conference, 1–5 October. Canada, Calgary, Alberta. https://doi.org/10.1115/IPC2000-175.

O'Donoghue, A.F., 1996. On the Steady State Motion of Conventional Pipeline Pigs Using Incompressible Drive Media. Cranfield University, PhD Dissertation.

Patricio, R.A.C., Baptista, R.M., de Freitas Rachid, F.B., Bodstein, G.C., 2020. Numerical simulation of pig motion in gas and liquid pipelines using the Flux-Corrected Transport method. J. Petrol. Sci. Eng. 189, 106970. https://doi.org/10.1016/j.petrol.2020.106970.

Persson, B.N., 2001. Theory of rubber friction and contact mechanics. J. Chem. Phys. 115 (8), 3840–3861. https://doi.org/10.1063/1.1388626.

Quarini, J., Shire, S., 2007. A review of fluid-driven pipeline pigs and their applications. Proc. IME E J. Process Mech. Eng. 221 (1), 1–10. https://doi.org/10.1243/0954408JPME108.

Rahe, F., 2006. Optimizing the active speed control unit for in-line inspection tools in gas. In: International Pipeline Conference, 25–29 September. Canada, Calgary, Alberta. https://doi.org/10.1115/IPC2006-10260.

Sadovnychiy, S., Lopez, J., 2005. Improvement of pipeline odometer system accuracy. In: Canadian International Petroleum Conference, 7–9 June. Canada, Calgary, Alberta. https://doi.org/10.2118/2005-013.

Saeidbakhsh, M., Rafeeyan, M., Ziaei-Rad, S., 2009. Dynamic analysis of small pigs in space pipelines. Oil & Gas Science and Technology-Revue de l'IFP. 64 (2), 155–164. https://doi.org/10.2516/ogst:2008046.

Tan, G.B., Wang, D.G., Liu, S.H., Zhang, S.W., 2014. Probing tribological properties of waxy oil in pipeline pigging with fluorescence technique. Tribol. Int. 71, 26–37. https://doi.org/10.1016/j.triboint.2013.10.020.

Tiratsoo, J., 1992. Pipeline Pigging Technology. Gulf Professional Publishing.

Tiratsoo, J., 2013. Pipeline Pigging & Integrity Technology. Clarion Technical Publishers.

Van Spronsen, G., Entaban, A., Mohamad Amin, K., Sarkar, S., Henkes, R.A.W.M., 2013. Field experience with by-pass pigging to mitigate liquid surge. In: International Conference on Multiphase Production Technology, 12–14 June, Cannes, France.

Zhang, H., Zhang, S., Liu, S., Wang, Y., Lin, L., 2015. Measurement and analysis of friction and dynamic characteristics of PIG's sealing disc passing through girth weld in oil and gas pipeline. Measurement 64, 112–122. https://doi.org/10.1016/

j.measurement.2014.12.046.
Zhang, Z., Yang, Y., Hou, J., Gong, Y., 2020. Modeling and simulation on speed prediction of bypass pipeline inspection gauge in medium of water and crude oil. Measurement and Control 53 (9–10), 1851–1860. https://doi.org/10.1177/0020294020947123.
Zhang, H., Gao, M., Tang, B., Cui, C., Xu, X., 2022. Dynamic characteristics of the pipeline inspection gauge under girth weld excitation in submarine pipeline. Petrol. Sci. 19 (2), 774–788. https://doi.org/10.1016/j.petsci.2021.09.044.
Zhu, X., Zhang, S., Li, X., Wang, D., Yu, D., 2015. Numerical simulation of contact force on bi-directional pig in gas pipeline: at the early stage of pigging. J. Nat. Gas Sci. Eng. 23, 127–138. https://doi.org/10.1016/j.jngse.2015.01.034.
Zhu, X., Wang, W., Zhang, S., Liu, S., 2017. Experimental research on the frictional resistance of fluid-driven pipeline robot with small size in gas pipeline. Tribol. Lett. 65 (2), 1–10. https://doi.org/10.1007/s11249-017-0830-z.